

# Computational and Experimental Analysis of Quercetin as a Potent Antibacterial Agent

Touhami Lanez<sup>1,\*</sup>, Elhafnaoui Lanez<sup>1</sup>, Aicha Adaika<sup>1</sup>, Kheira Lammari<sup>1</sup>

<sup>1</sup> University of El Oued, VTRS laboratory, Faculty of Sciences, B.P.789, 39000, El Oued, Algeria

\* Correspondence: [touhami-lanez@univ-eloued.dz](mailto:touhami-lanez@univ-eloued.dz);

Received: 20.09.2024; Accepted: 21.07.2025; Published: 30.09.2025

**Abstract:** This study focuses on the antibacterial activity of a series of quercetin analogs against *Escherichia coli* using both *in vitro* and *in silico* methods. A combinatorial library of 1475 quercetin analogs was generated using SmiLib software, and all analogs were subjected to rigorous virtual screening to evaluate their toxicity and ADMET properties. Three candidates with the lowest toxicity and the most favorable ADMET profiles were selected for further evaluation using molecular docking and dynamics simulations to assess their antibacterial efficacy. *In vitro* results confirmed quercetin's significant antibacterial activity, while *in silico* simulations provided insights into the strong binding interactions and structural stability of quercetin analogs with the Estrogen receptor of the bacterial targets "*Escherichia coli*". The study demonstrated that selected analogs possessed promising potential as antibacterial agents.

**Keywords:** *Escherichia coli*; flavonoids; IC<sub>50</sub>; *in silico*; molecular docking; molecular dynamics.

© 2025 by the authors. This article is an open-access article distributed under the terms and conditions of the Creative Commons Attribution (CC BY) license (<https://creativecommons.org/licenses/by/4.0/>), which permits unrestricted use, distribution, and reproduction in any medium, provided the original work is properly cited. The authors retain copyright of their work, and no permission is required from the authors or the publisher to reuse or distribute this article, as long as proper attribution is given to the original source.

## 1. Introduction

Antibiotic resistance is a big global health issue that is growing over time, which has made it hard to treat patients with bacterial infections using normal antibiotics [1,2]. The prevailing practices of irrational usage or abuse of antibiotics in healthcare and farming have facilitated the emergence of superbugs, creating an urgent need for novel treatment options [3]. The World Health Organization stated that out of the threats to human health facing the world in recent years, antibiotic resistance is the greatest, at least in the twenty-first century [4]. This is particularly worrisome as it raises the importance of identifying new classes of antibiotics, especially those from natural products, that would be safer and more environmentally considerate than synthetic ones.

Flavonoids, which are polyphenolic compounds from plants, have at their disposal a very fair range of biological activities for which they have been read: antioxidants [5], anti-inflammatory [6,7], and antimicrobial activities [8,9]. Quercetin is one of the best-known classes of advanced and studied flavonoids [10-14]. Quercetin-rich compounds are widely available throughout fruits, vegetables, and certain functional foods, such as onions, apples, berries, and leafy greens [15]. There is ample evidence to support the claim that quercetin's pharmacological effects are health-promoting, such as scavenging of free radicals [16-18], inhibition of inflammatory response, and prevention of cancer cell proliferation [19-22]. The

recent and current efforts have also shown the use of quercetin as an antibacterial agent, and this opens a possibility of quercetin in a new application of solving the problem of antibiotic resistance [23,24].

Notably, the action of quercetin on bacterial cells remains obscure, yet most researchers acknowledge its antibacterial value [25]. Even so, it is taken into the body after being administered treatment, and movement to specific localized areas is a barrier. In order to overcome these challenges and improve its antibacterial activity, scientists have begun studying the structural modifications of quercetin, aiming at the creation of new derivatives with better pharmacological profiles [26]. Through changing its chemical profile, it is possible to enhance its effectiveness in targeting bacterial agents while minimizing potential side effects.

With respect to this nagging concern, the present work emphasizes the biodelimiting action of quercetin polyphenol and its derivatives against *Escherichia coli*, a generally associated pathogen linked with various forms of infections. Review of quercetin derivatives for their capacity to inhibit the bacterial activity of microorganisms combines these techniques in vitro and in silico. In vitro assays like the disc diffusion assay, which employs agar plates, were also performed to directly test the antibacterial property of quercetin. Whereas in silico molecular docking and molecular dynamics simulations, which target the relative binding positions of the compounds and the stability of their structures in contact with bacterial proteins, are applied.

By systematically modifying the chemical structure of quercetin and evaluating the resulting derivatives, we aim to identify compounds with enhanced antibacterial properties. Additionally, the integration of in silico simulations provides valuable insights into the molecular interactions between quercetin analogs and bacterial targets, helping to elucidate their mechanisms of action. This combined approach offers a promising strategy for the discovery and development of new antibacterial agents that could potentially address the growing issue of antibiotic resistance.

## 2. Materials and Methods

### 2.1. Chemicals.

Quercetin, Dimethyl sulfoxide, sodium chloride, Agar medium, Nutrient broth, Mueller-Hinton agar, and gentamicin were obtained from Sigma-Aldrich and used as received. All other reagents and solvents used in the research were analytical grade and procured from different commercial sources without any further purification. All solutions used here were prepared using doubly distilled water. All results shown in this study are the average of three independent experimental measurements.

### 2.2. Biological materials, instruments, and software.

The microorganism used for antimicrobial activity evaluation was *Escherichia coli* (ATCC 25922), a Gram-negative bacillus from the Enterobacteriaceae family. UV spectrophotometer (UV-1800 SHIMADZU) with a 2 mL cell of 10 mm optical path length, Centrifuge, Water bath, LAB TECH type incubator, Antibiotic discs. The tools used for in silico screening include Gauss View 6.0, Smilib 2, with web servers SwissADME and pkcsm.

### 2.3. *In vitro* evaluation of antibacterial activity.

#### 2.3.1. Preparation of test sample and research protocol.

Quercetin was dissolved in DMSO to prepare solutions with concentrations ranging from 0.0125 to 2 mg/mL. The antibacterial activity was determined using the disc diffusion method. The surface of the agar plates was inoculated with the bacterial strains under study. After incubation, the maximum inhibitory concentration of *Escherichia coli* was determined by observing the growth inhibition on the medium with the lowest quercetin concentration.

#### 2.3.2. Strain preservation and preparation of pre-cultures.

Strains were preserved at 5°C in sterile tubes containing 10 mL of inclined nutrient agar medium. Microbial strains were cultured on Petri dishes containing nutrient agar and incubated for 24 hours at 37°C to obtain young cultures and isolated colonies.

#### 2.3.3. Preparation of discs and bacterial suspensions.

Discs were prepared using 6 mm diameter Whatman filter paper, sterilized for 30 minutes at 120°C in the autoclave, and stored until use. Several well-isolated colonies were picked with a Pasteur pipette and placed in 10 mL of sterile physiological saline (0.9% NaCl). The bacterial suspension was standardized to 0.5 McFarland ( $1.5 \times 10^8$  CFU/ml) using a densitometer.

#### 2.3.4. Antibacterial activity test.

Sterile Mueller-Hinton agar was poured into Petri dishes to a 4 mm thickness and allowed to solidify. The bacterial suspension was spread evenly over the surface using a sterile swab and left for 30 minutes. Antibacterial activity was determined by measuring the inhibition zone diameter using a ruler, compared with DMSO (negative control) and antibiotics (positive control, Gentamicin 120 µg/disc), and by measuring absorbance using UV-vis spectroscopy.

### 2.4. *In silico* evaluation of antibacterial activity.

The *in silico* antibacterial activity of selected quercetin analogs was carried out using receptor ID: PDB 1R20 and was performed on a personal computer with the following specifications: Intel(R) Core (TM) i5-6440HQ CPU @ 2.60GHz, 8.00 GB RAM, running Windows 10 Pro.

### 2.5. Generation of combinatorial library.

SmiLib v2.0 software [27] was used to numerate quercetin analogs using the quercetin structure as a scaffold and the functional groups (NO<sub>2</sub>, Cl, C<sub>2</sub>H<sub>5</sub>, NH<sub>2</sub>, and F) along with vacant linkers.

### 2.6. Molecular docking simulations.

Molecular docking simulations were carried out using the Schrödinger Maestro software package [28]. This is a rather involved process of predicting the binding modes and affinities of ligands to protein targets.

### 3. Results and Discussion

The antimicrobial activity of quercetin is assessed by the minimum inhibitory concentration (IC<sub>50</sub>) in μM, where a lower IC<sub>50</sub> value indicates stronger antimicrobial activity, comparable to amoxicillin as a reference drug Table 1.

**Table 1.** Diameters of zones of inhibition and absorbency of bacteria.

C (mg/ml)	2	1	0.8	0.6	0.4	0.2	0.025	0.0125
Diameter (mm)	10	9.5	9	9	9	10	9.5	8.5
Absorbance (u.a)	0.321	0.323	0.338	0.449	0.459	0.517	0.868	0.988
Inhibition (%)	83.96	83.86	83.11	77.57	77.07	74.17	56.54	50.54

The IC<sub>50</sub> was calculated from the equation obtained from the regression plot of the percent of inhibition versus quercetin concentration presented in Figure 1. The IC<sub>50</sub> value, which represents the concentration of quercetin required to inhibit 50% of bacterial growth, was calculated based on the data provided for the percentage of inhibition at varying concentrations of quercetin. The regression equation was derived from the plot of percentage inhibition versus quercetin concentration (as shown in Figure 1).

The calculated IC<sub>50</sub> value is 12.8 μM, indicating a highly potent inhibitory effect of quercetin at a relatively low concentration. This value is in line with the trend observed in the experimental data [29,30], where inhibition remains consistently high across most concentrations, gradually decreasing at lower quercetin concentrations. The strong correlation between concentration and inhibition percentage further supports the robustness of this IC<sub>50</sub> calculation.

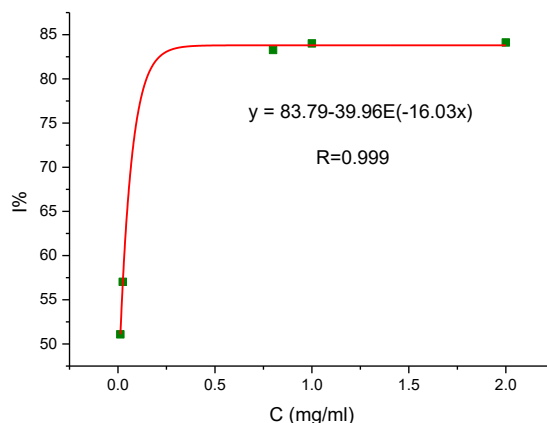


**Figure 1.** Plot of percentage of inhibition versus quercetin concentration used to calculate IC<sub>50</sub>.

The IC<sub>50</sub> value of the reference drug amoxicillin was also measured under the same experimental conditions as that of quercetin (data not presented), ensuring a reliable and consistent comparison between the two compounds. The fact that both compounds were evaluated using the same methodology confirms that the observed difference in potency is due to their inherent biological activity rather than experimental variability.

The IC<sub>50</sub> value of quercetin (12.8 μM) compared to that of the reference drug amoxicillin (8.1 μM) indicates that quercetin has a somewhat lower but comparable antibacterial potency against the tested bacterial strain. While amoxicillin, a well-established antibiotic, exhibits stronger inhibitory activity with a lower IC<sub>50</sub> value, quercetin's value is still within a reasonable range for antibacterial agents derived from natural compounds.

This slight difference in IC<sub>50</sub> may be attributed to the distinct mechanisms of action between the two compounds. Amoxicillin disrupts bacterial cell wall synthesis, which is a

highly effective and targeted mechanism. In contrast, quercetin exerts its antibacterial effects through multiple pathways, such as disruption of the bacterial membrane, inhibition of enzymes, or interference with bacterial DNA, which may result in a slightly higher IC<sub>50</sub>.

Despite the higher IC<sub>50</sub> value, quercetin's broad-spectrum biological activities, including its antioxidant and anti-inflammatory properties, make it an attractive natural alternative or adjunct to traditional antibiotics like amoxicillin, especially in the context of increasing antibiotic resistance. Further modifications of quercetin derivatives may improve their antibacterial efficacy and bring their IC<sub>50</sub> value closer to or even higher than that of amoxicillin.

The binding constant K<sub>b</sub> was determined from the absorption data according to the Benesi-Hildebrand equation (1) [31,32].

$$\frac{A_0}{A-A_0} = \frac{\epsilon_f}{\epsilon_b-\epsilon_f} + \frac{\epsilon_f}{\epsilon_b-\epsilon_f} \frac{1}{K_b C} \quad (1)$$

In equation (1), A<sub>0</sub> and A are the absorbencies of *Escherichia coli* in the presence and absence of quercetin, respectively, while  $\epsilon_f$  and  $\epsilon_b$  are their extinction coefficients. A plot of A<sub>0</sub>/(A-A<sub>0</sub>) versus 1/C gave a slope of  $\epsilon_f/(\epsilon_b-\epsilon_f)K_b$  and a 'y' intercept equal to  $\epsilon_f/(\epsilon_b-\epsilon_f)$ , where K<sub>b</sub> is the ratio of the slope to the y intercept, Figure 2. The obtained value of the binding constant is  $6.48 \times 10^4 \text{ M}^{-1}$ , and its corresponding free binding energy calculated using the equation ( $\Delta G = -nRT \ln K_b$ ) is equal to  $-6.53 \text{ kcal mol}^{-1}$ . These values suggest a strong binding affinity between quercetin and the bacterial receptor EcR.

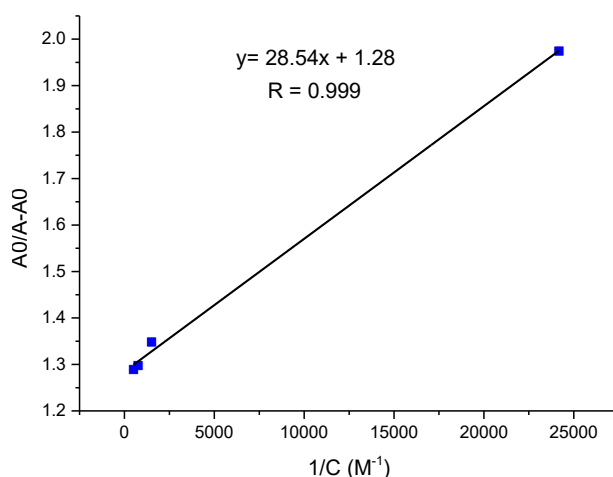


**Figure 2.** Plot of 1/C versus A<sub>0</sub>/(A-A<sub>0</sub>) used to calculate the binding constant between quercetin and *Escherichia coli*.

### 3.1. Virtual screening.

The building blocks used were the scaffold structure shown in Figure 3. The SMILES structures of both the scaffold and the functional groups were added to the SmiLib interface. Using this method, a large library of compounds was constructed in SMILES format, containing 1475 quercetin analogs.

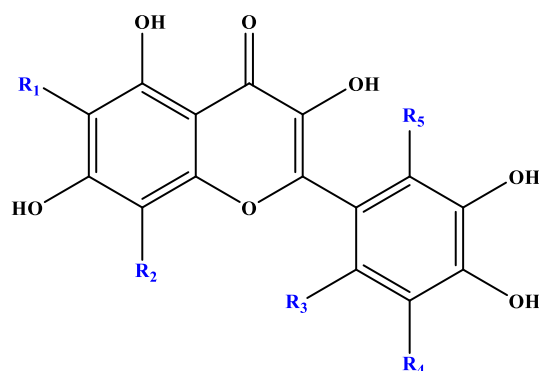


**Figure 3.** Scaffold structure used for the enumeration of quercetine analogues.

All enumerated molecules underwent thorough virtual screening to determine their lethal dose (LD<sub>50</sub>) using the pkCSM online web server [33]. Molecules exhibiting lower toxicity compared to quercetin were selected for further analysis. The selected analogues then underwent comprehensive ADMET virtual screening to assess their physicochemical properties, drug-likeness, pharmacokinetics, and medicinal chemistry profiles. Molecules that exhibit unfavorable properties were eliminated from further investigation. This screening identified analogs Q4, Q7, and Q8 as promising candidates, meriting further investigation through molecular docking and molecular dynamics studies. ADMET profiles of the promising candidates and the reference drug amoxicillin are presented in Figure 4.

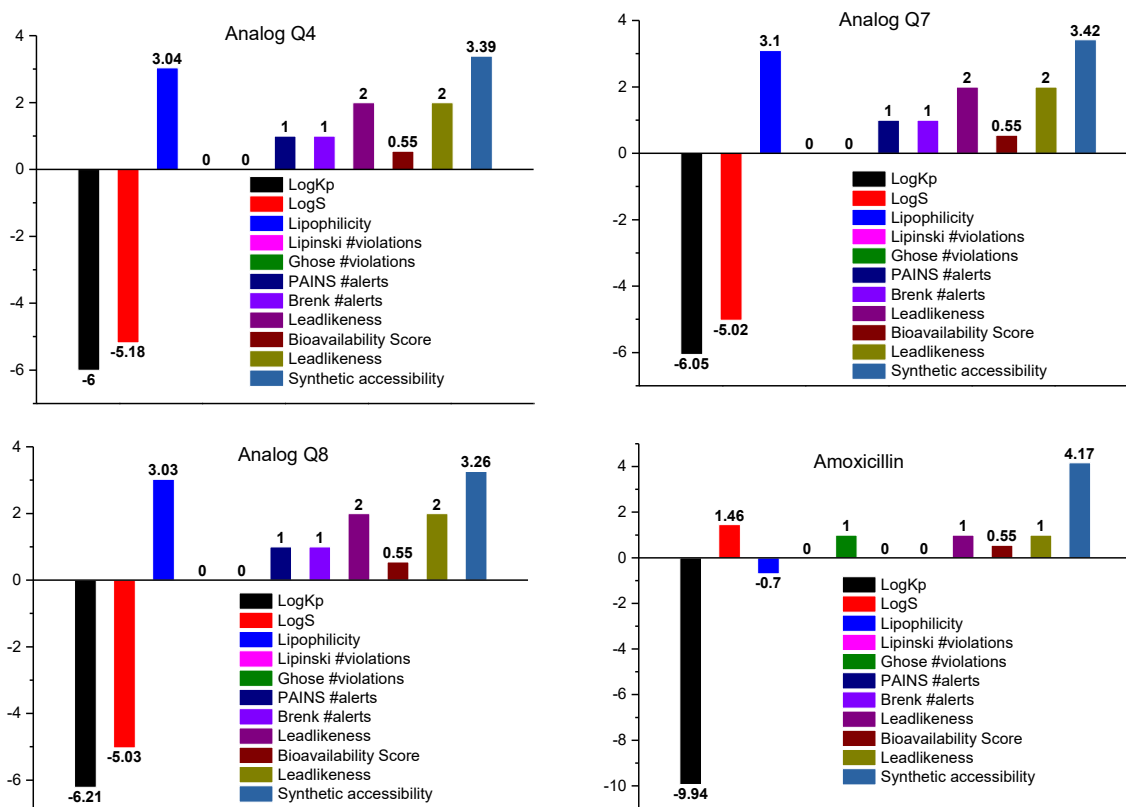


**Figure 4.** ADMET profiles of analogs Q4, Q7, Q8, and the reference drug amoxicillin.

### 3.2. Molecular docking.

The crystal structure of the protein of the heterodimer EcR chosen for investigation in molecular docking studies was obtained from the protein data bank (RCSB, PDB ID: 1R20), Figure 5. The Receptor Grid was then created to define the interaction area of the protein and the ligand. This was done with the Receptor Grid Generation tool of Maestro, by specifying

the box around the active site using its (x,y,z) coordinates. For the receptors, the number of grid points was 20 along each of the x, y, and z dimensions, which correspond to the x, y, and z axes, respectively. All docking analysis was performed using the Glide program in Maestro [34].

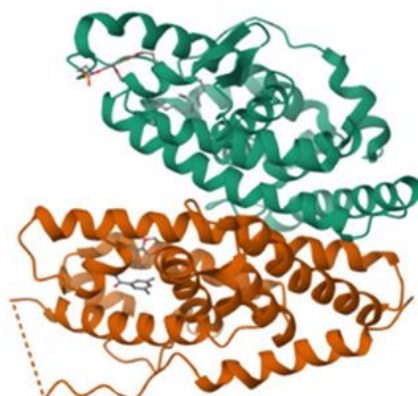


**Figure 5.** Three-dimensional structure of EcR receptor of *Escherichia coli* (1R20) bound to the synthetic agonist BYI06830.

### 3.2.1. Ramachandran plot results.

The Ramachandran plot and its corresponding statistics were obtained from the web server (<https://saves.mbi.ucla.edu/>) [35,36]. The protein 1R20 A plots were analyzed, and their statistical details are provided in Table 2. Based on the Ramachandran plot statistics, the three-dimensional structure with PDB ID: 1R20 has 80% of its residues in favorable regions, 17.6% in additionally allowed regions, 1.4% in generously allowed regions, and 0.0% in disallowed regions. These values strongly support the quality and the stability of the protein chosen for molecular docking and molecular dynamics simulations, which is suitable to provide the highest docking score and lowest RMSD values with quercetin. The plot is illustrated in Figure 6.

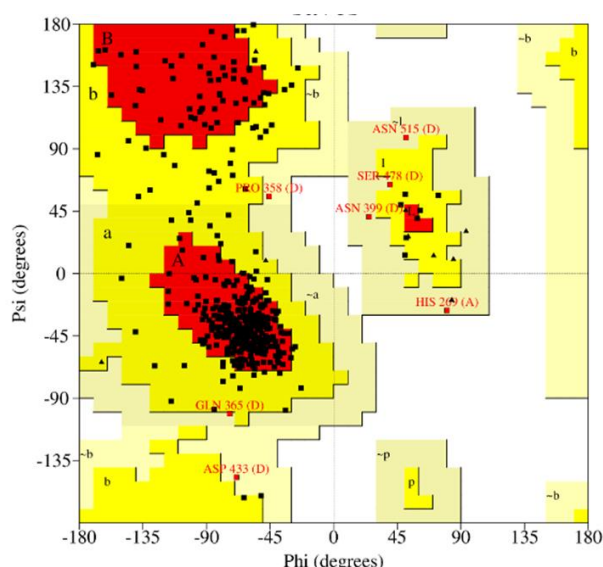


**Figure 6.** Structure authentication using the (A) Ramachandran strategy; (B) Ramachandran plot indicators of the 1R20 protein.

**Table 2.** Ramachandran plot statistics of residues of 1R20.

Residues in the most favored regions	Residues in additional allowed regions	Residues in generously allowed regions	Residues in disallowed regions	Number of non-glycine and non-proline residues	No of end-residues	No of glycine residues	No of proline residues	Total no of residues
341=80.0%	74=17.6%	6=1.4%	0=0.0%	421=100.0%	8	17	21	467

### 3.2.2. Geometry optimization.

Obtaining the optimized structure of small molecules is very crucial for elucidating their exact binding behavior. Therefore, to comprehensively understand this behavior, the structures of the highly potent analogs Q4, Q7, and Q8, along with quercetin, were fully optimized using the DFT/B3LYP method as outlined in the experimental and computational details section. The resulting optimized ground state geometries of these compounds are depicted in Figure 7.

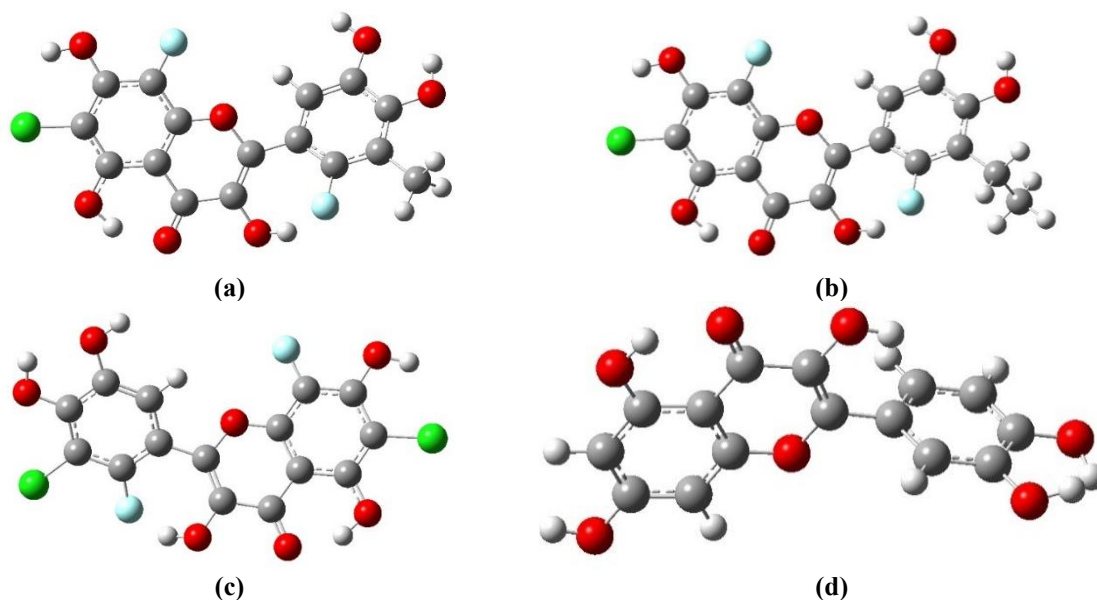


**Figure 7.** The optimized 3D-structure of analog (a) Q4; (b) Q7; (c) Q8; (d) quercetin at the DFT/B3LYP method.

### 3.2.3. Molecular docking results.

In order to explain how the most active quercetin analogs, Q4, Q7, and Q8, along with the parent compound quercetin, interact with the receptors EcR of *Escherichia coli*, molecular docking studies were carried out; these simulations are used to determine the most stable conformation of the compounds when docked to the chosen target receptor. The docking analysis depicted in Figure 8 provides deeper insights into the 2D interaction modes of the tested compounds within the binding site of the EcR receptor. The key amino acid residues that interact with quercetin and its analogs include ASN504 and THR340, which are conserved binding sites. The red lines are hydrogen bonds between the ligands and the receptor. As shown in Figure 8, quercetin and all of the other analogs make two hydrogen bonds with the residues ASN504 and THR340 of the receptor EcR, except for analog Q7. Other nearby residues (VAL416, CYS508, and MET381) are also positioned to make hydrophobic and van der Waals interactions, which could also help to stabilize the ligand-receptor complex.

Table 3 presents an analysis of the bond interactions and binding free energies for three quercetin analogs (Q4, Q7, and Q8) and quercetin itself, in their interactions with the EcR receptor. All ligands consistently interact with two key residues, ASN504 and THR340, suggesting these residues are crucial for ligand binding. Analog Q7 shows an additional interaction with SER377, which may contribute to its slightly higher binding affinity. The bond distances between the ligands and interacting residues are given in angstroms (Å), with shorter distances generally indicating stronger interactions.

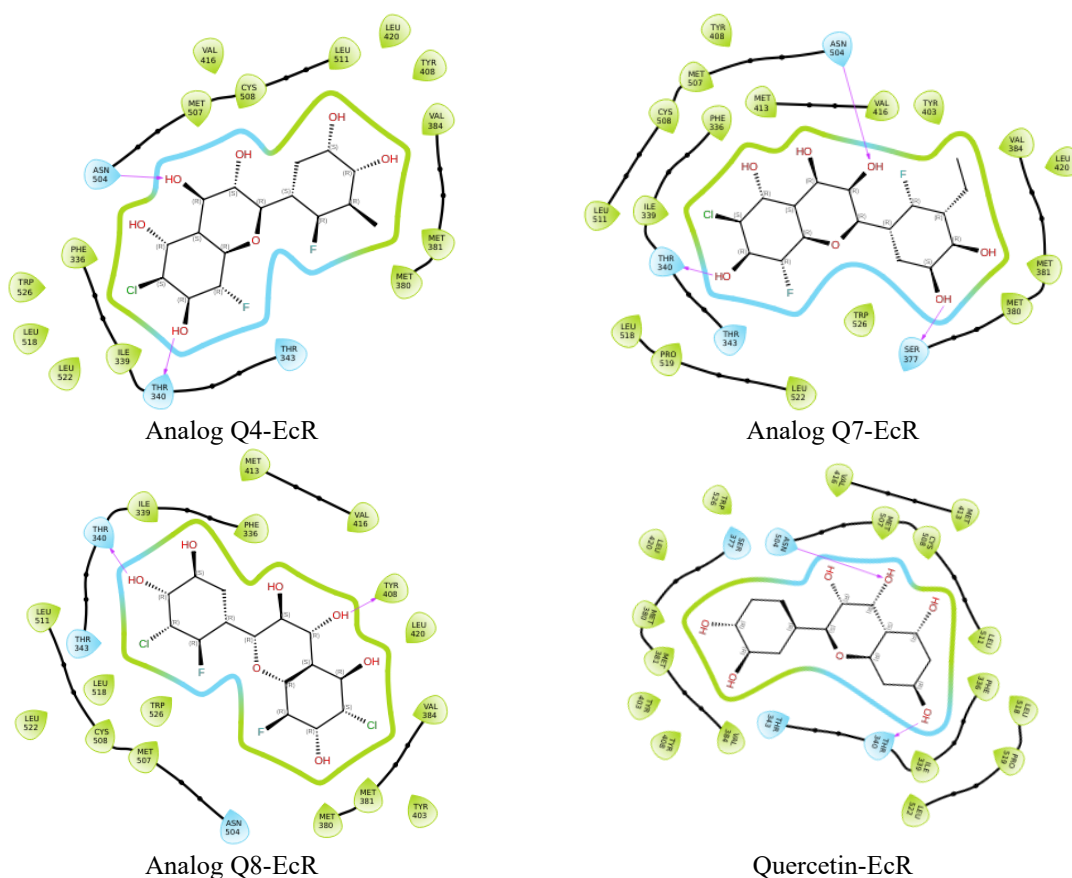


**Figure 8.** 2D interaction of quercetin analogues with the target EcR of *Escherichia coli*, where the red lines represent the H-bonds.

The shortest bond distance (1.40 Å) is seen between analog Q4 and THR340, implying a strong interaction. In contrast, the bond distances between SER377 in analog Q7 and THR408 in analog Q8 are longer, suggesting comparatively weaker interactions. The binding free energies reflect the strength of the ligand-receptor interactions, with more negative values corresponding to stronger affinities. Quercetin (-9.78 kcalmol<sup>-1</sup>) demonstrates a slightly stronger binding affinity than analog Q4 (-9.23 kcalmol<sup>-1</sup>) and analog Q8 (-8.88 kcalmol<sup>-1</sup>), while analog Q7 exhibits the strongest binding affinity (-9.63 kcalmol<sup>-1</sup>), likely due to its additional interaction with SER377.

**Table 3.** Bond interactions analysis and binding free energies of Analogs Q4, Q7, Q8, and quercetin, candidates with the receptor EcR.

Ligand	Interacting residues	Distance (Å)	-ΔG(kcalmol <sup>-1</sup> )
Analog Q4	ASN504	2.00	9.23
	THR340	1.40	
Analog Q7	ASN504	2.48	9.63
	THR340	1.96	
Analog Q8	SER377	2.44	8.88
	THR340	2.00	
Quercetin	THR408	1.75	9.78
	ASN504	2.11	
	THR340	1.74	

### 3.2.4. Docking validation.

The docking procedure was validated by redocking the co-crystallized ligand named N-(tert-butyl)-3,5-dimethyl-N'-[(5-methyl-2,3-dihydro-1,4-benzodioxin-6-yl) carbonyl]benzohydrazide to the EcR protein structure using the same approach that was used for quercetin and its analogs.

The co-crystallized ligand was first separated from the protein structure and then docked into the same protein. To this end, the redocked co-crystallized ligand and its crystalline form were superimposed. Figure 9 presents a superimposed view of the redocked conformation (golden color) and the original ligand (green color); the calculated RMSD value between them is 0.33 Å. The clear superimposition between both ligands and the RMSD value is less than 2 Å, which confirms the correctness of the grid box determined for the docking and how effective the algorithms are at performing the molecular docking protocol.

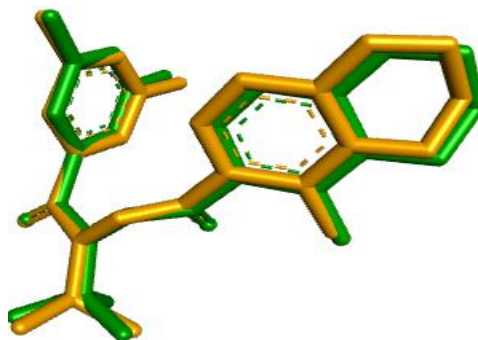


**Figure 9.** Superimposed crystal ligand (in green) and redocked ligand (in gold) with an RMSD value of 0.33 Å.

### 3.3. Molecular dynamics simulation study.

Molecular Dynamics simulations were carried out using the Desmond software to rigorously examine the stability of the protein-ligand complexes in a physiological environment. The duration of the molecular dynamic simulations spanned 100 nanoseconds, allowing for a comprehensive analysis of the behavior exhibited by the candidate ligand molecules within the binding sites of the EcR receptor. During the molecular dynamics simulations, many important parameters such as Root Mean Square Deviation (RMSD), Root Mean Square Fluctuation (RMSF), and radius of gyration were tracked from trajectory data. These parameters served as indispensable metrics for meticulously evaluating the stability and binding affinity of the protein-ligand complexes within dynamic environments.

#### 3.3.1. Root mean square deviation.

To determine the stability of the protein-ligand complexes that formed with the chosen quercetin analogs, the root mean square deviation of the carbon alpha atoms was computed, and the results are shown in Figure 10. The RMSD values of all studied complexes remain below 2 angstroms, but for the complexes analog Q4-EcR and analog Q7-EcR, the RMSD values increased to values above 3 angstroms and stayed at that level for the rest of the simulation. The RMSD of the complex analog Q8-EcR exhibited significant deviations throughout the simulation, which indicates the instability of this analog Q8-EcR complex. From the resulting RMSD values, all analogues are most likely candidates as anti-bacterial agents, and they are even more stable than the control quercetin.

#### 3.3.2. Root mean square fluctuation.

To assess the mobility of the protein when in complex with the ligands, we determined the root mean square fluctuations (RMSF). These values represent the amount of flexibility and movement of individual protein residues over the entire length of the simulation.

When we looked at the RMSF values for the protein EcR, we found that most of the residues in the protein barely moved more than 2 angstroms during the entire simulation. This

suggests that these residues maintained a relatively rigid and stable conformation in the presence of the studied ligands. However, the loop regions of the protein demonstrated higher RMSF values, peaking at approximately 3.5 Å Figure 11.

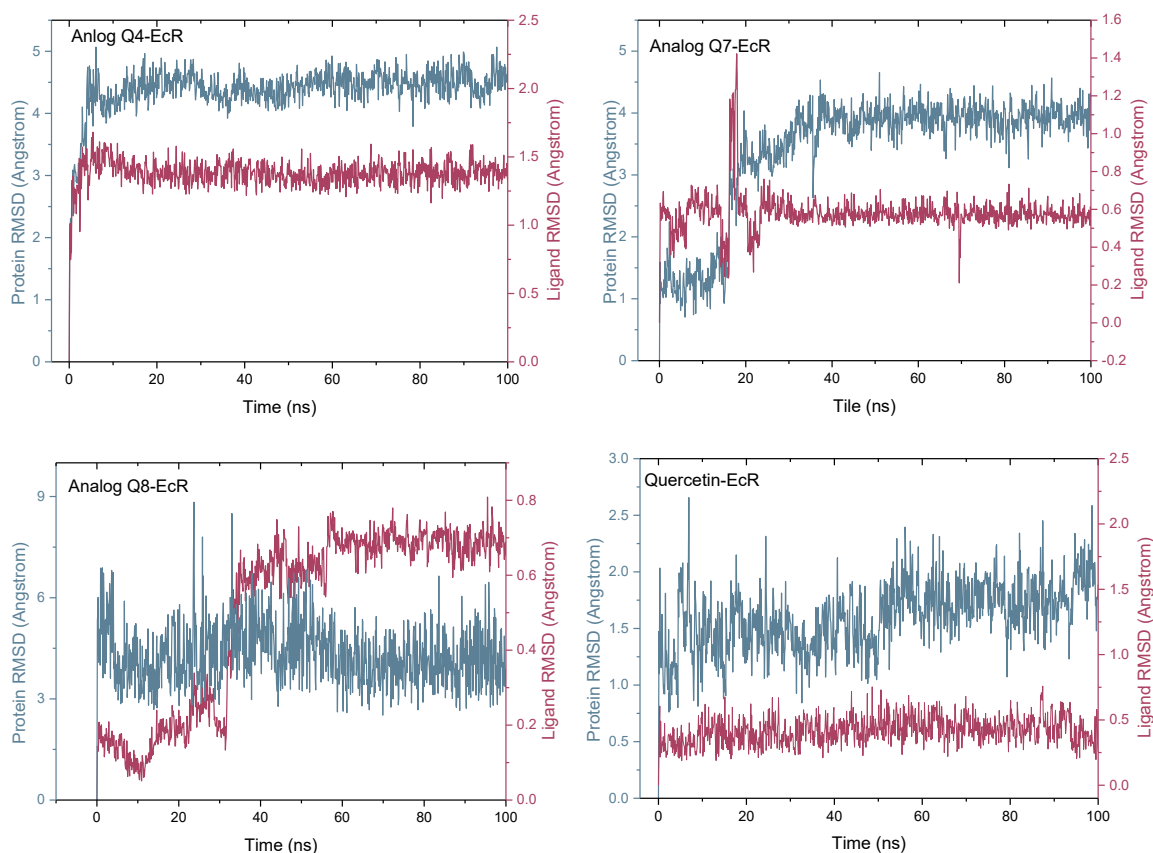


**Figure 10.** The RMSD plots of protein complexes during a 100 ns simulation of the selected candidates, along with the quercetin.

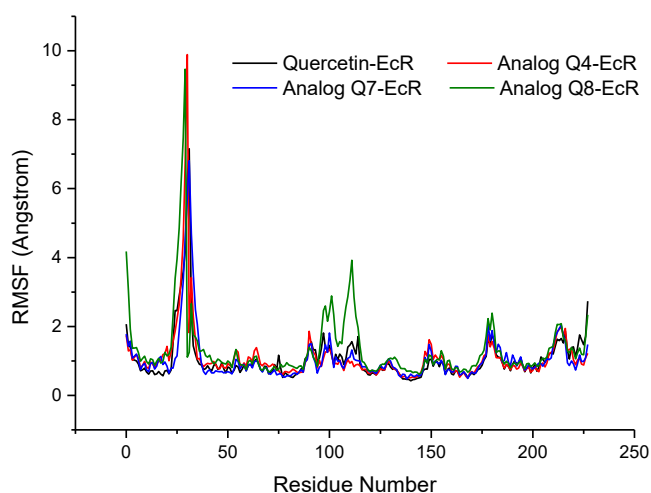


**Figure 11.** The fluctuation of protein residues of EcR during simulations as determined by RSMF values.

### 3.3.3. Radius of gyration.

To evaluate the structural compactness of the EcR protein in complex with the selected compounds, along with quercetin, we conducted an analysis of the radius of gyration (Rg). The Rg values provide insights into the overall compactness of the protein structure, where lower values indicate a more compact structure and higher values suggest unfolding events during the simulation. The Rg plots of the ligands-EcR complexes revealed that the Rg values

remained stable within the range of 3.8 to 4.3 Å throughout the simulation (Figure 12). This indicates that the protein structure maintained its compact conformation when bound to the studied compounds. The consistent Rg values further support the notion of structural stability during the simulation period.

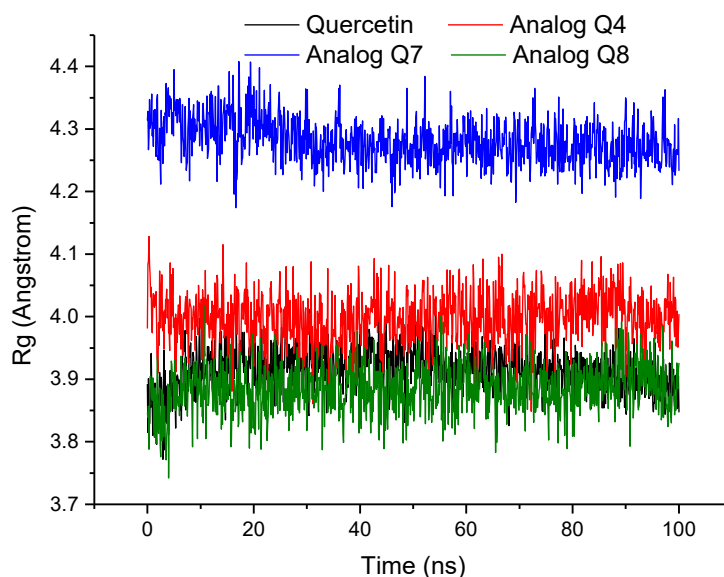


**Figure 12.** The Rg plots of quercetin-EcR-, analog Q4-EcR, analog Q7-EcR, and analog Q8-EcR complexes as a function of simulation time.

The outcomes of the virtual screening investigation and molecular docking study revealed the ranking of antibacterial activity as follows: analog Q7 > analog Q4 > analog Q8. Conversely, molecular dynamics simulation also indicated the same order of complex stability: analog Q7-EcR > analog Q4-EcR > analog Q8-EcR. Taking into account these collective findings, the analog Q7 emerges as a noteworthy candidate.

#### 4. Conclusions

In this work, we investigated the antibacterial efficacy of quercetin and its analogs against *Escherichia coli*, combining *in vitro* and *in silico* approaches. The obtained results showed that quercetin has substantial inhibitory activity ( $IC_{50} = 12.8 \mu\text{M}$ ), almost comparable to that of the reference drug amoxicillin ( $IC_{50} = 8.1 \mu\text{M}$ ). Molecular docking analysis revealed that quercetin and its selected analogs have strong binding affinities, mainly attributed to the important interactions they have with the residues ASN504 and THR340 of the receptor EcR of *Escherichia coli* (1R20). Among the tested analogs, Q7 exhibited the highest binding affinity due to its additional hydrogen bond formation with SER377. The integration of molecular dynamics simulations provided critical insights into the structural stability of the quercetin analog-receptor complexes. The findings suggest that quercetin derivatives hold potential as alternative antibacterial agents, offering a natural solution to combat antibiotic resistance.

#### Author Contributions

Conceptualization, T. L. and E. L.; Methodology, T. L.; Software, T. L.; Validation, T. L., E. L., and A. A.; Formal analysis, T. L.; Investigation, A. A. and K. L.; Resources, T. L.; Data curation, E. L.; Writing—original draft preparation, T. L.; Writing—review and editing, T. L.

and K. L.; Visualization, E. L.; Supervision, T. L.; Project administration, T. L.; Funding acquisition, T. L.. All authors have read and agreed to the published version of the manuscript.

### **Institutional Review Board Statement**

Not applicable.

### **Informed Consent Statement**

Not applicable.

### **Data Availability Statement**

No new data were created or analyzed in this study. Data sharing is not applicable.

### **Funding**

This research received no external funding.

### **Acknowledgments**

The authors are grateful to the Algerian Ministry of Higher Education and Research for financial support (project code: B00L01UN390120150001).

### **Conflicts of Interest**

The authors declare no conflict of interest.

### **References**

1. Berardi, A.; Zinani, I.; Rossi, C.; Spaggiari, E.; D'Amico, V.; Toni, G.; Bedetti, L.; Lucaccioni, L.; Iughetti, L.; Lugli, L. Antibiotic Use in Very Low Birth Weight Neonates After an Antimicrobial Stewardship Program. *Antibiotics* **2021**, *10*, 411, <https://doi.org/10.3390/antibiotics10040411>.
2. Murray, C. J. L.; Ikuta, K. S.; Sharara, F.; Swetschinski, L.; Robles Aguilar, G.; Gray, A.; Han, C.; Bisignano, C.; Rao, P.; Wool, E.; Johnson, S. C.; Browne, A. J.; Chipeta, M. G.; Fell, F.; Hackett, S.; Haines-Woodhouse, G.; Kashef Hamadani, B. H.; Kumaran, E. A. P., McManigal, B.; Naghavi, M. Global burden of bacterial antimicrobial resistance in 2019: a systematic analysis. *Lancet* **2022**, *399*, 629–655, [https://doi.org/10.1016/s0140-6736\(21\)02724-0](https://doi.org/10.1016/s0140-6736(21)02724-0).
3. Nthumba, P. M. Effective Hand Preparation for Surgical Procedures in Low- and Middle-Income Countries. *Surg. Infect.* **2020**, *21*, 495–500, <https://doi.org/10.1089/sur.2020.025>.
4. Global Antimicrobial Resistance and Use Surveillance System (GLASS) Report: **2021**. Available online: <https://www.who.int/publications/i/item/9789240027336> (accessed on 17 July **2024**).
5. Byun, K.A.; Oh, S.; Son, M.; Oh, S. E.; Park, C.-H.; Son, K. H.; Byun, K. Dieckol-Attenuated High-Fat Diet Induced Muscle Atrophy by Modulating Muscular Deposition of Lipid Droplets. *Nutrients* **2021**, *13*, 3160, <https://doi.org/10.3390/nu13093160>.
6. Al-Khayri, J.M.; Sahana, G.R.; Nagella, P.; Joseph, B.V.; Alessa, F.M.; Al-Mssallem, M.Q. Flavonoids as Potential Anti-Inflammatory Molecules: A Review. *Molecules* **2022**, *27*, 2901, <https://doi.org/10.3390/molecules27092901>.
7. Ysrafil, Y.; Sapiun, Z.; Slamet, N.S.; Mohamad, F.; Hartati, H.; Damiti S.A.; Alexandra, F.D.; Rahman, S.; Masyeni, S.; Harapan, H.; Mamada, S.S.; Bin Emran, T.; Nainu, F. Anti-inflammatory activities of flavonoid derivatives. *ADMET DMPK* **2023**, *11*, 331-359, <https://doi.org/10.5599/admet.1918>.
8. Thebti, A.; Meddeb, A.; Ben Salem, I.; Bakary, C.; Ayari, S.; Rezgui, F.; Essafi-Benkhadir, K.; Boudabous, A.; Ouzari, H. Antimicrobial Activities and Mode of Flavonoid Actions. *Antibiotics* **2023**, *12*, 225, <https://doi.org/10.3390/antibiotics12020225>.

9. Yan, Y.; Xia, X.; Fatima, A.; Zhang, L.; Yuan, G.; Lian, F.; Wang, Y. Antibacterial Activity and Mechanisms of Plant Flavonoids against Gram-Negative Bacteria Based on the Antibacterial Statistical Model. *Pharmaceuticals* **2024**, *17*, 292, <https://doi.org/10.3390/ph17030292>.
10. Azeem, M.; Hanif, M.; Mahmood, K.; Ameer, N.; Chughtai, F.R.S.; Abid, U. An insight into anticancer, antioxidant, antimicrobial, antidiabetic and anti-inflammatory effects of quercetin: a review. *Polym. Bull.* **2023**, *80*, 241–262, <https://doi.org/10.1007/s00289-022-04091-8>.
11. Rajesh, R.U.; Dhanaraj, S.A. Critical review on quercetin bioflavonoid and its derivatives: Scope, synthesis, and biological applications with future prospects. *Arab. J. Chem.* **2023**, *16*, 104881, <https://doi.org/10.1016/j.arabjc.2023.104881>.
12. Deepika; Maurya, P.K. Health Benefits of Quercetin in Age-Related Diseases. *Molecules* **2022**, *27*, 2498, <https://doi.org/10.3390/molecules27082498>.
13. Aghababaei, F.; Hadidi, M. Recent Advances in Potential Health Benefits of Quercetin. *Pharmaceuticals* **2023**, *16*, 1020, <https://doi.org/10.3390/ph16071020>.
14. Carrillo-Martinez, E.J.; Flores-Hernández, F.Y.; Salazar-Montes, A.M.; Nario-Chaidez, H.F.; Hernández-Ortega, L.D. Quercetin, a Flavonoid with Great Pharmacological Capacity. *Molecules* **2024**, *29*, 1000, <https://doi.org/10.3390/molecules29051000>.
15. Yang, C.; Sun, N.; Qin, X.; Liu, Y.; Sui, M.; Zhang, Y.; Hu, Y.; Mao, Y.; Shen, X. Analysis of flavonoid metabolism of compounds in succulent fruits and leaves of three different colors of Rosaceae. *Sci. Rep.* **2024**, *14*, 4933, <https://doi.org/10.1038/s41598-024-55541-4>.
16. Vásquez-Espinal, A.; Yañez, O.; Osorio, E.; Areche, C.; García-Beltrán, O.; Ruiz, L. M.; Cassels, B. K.; Tiznado, W. Theoretical Study of the Antioxidant Activity of Quercetin Oxidation Products. *Front. Chem.* **2019**, *7*, 818, <https://doi.org/10.3389/fchem.2019.00818>.
17. Amić, A.; Mastil'ák Cagardová, D. A DFT Study on the Kinetics of HOO•, CH<sub>3</sub>OO•, and O<sub>2</sub>•-Scavenging by Quercetin and Flavonoid Catecholic Metabolites. *Antioxidants* **2023**, *12*, 1154, <https://doi.org/10.3390/antiox12061154>.
18. Chaudhary, P.; Janmeda, P.; Docea, A. O.; Yeskalyeva, B.; Abdull Razis, A. F.; Modu, B.; Calina, D.; Sharifi-Rad, J. Oxidative stress, free radicals and antioxidants: potential crosstalk in the pathophysiology of human diseases. *Front. Chem.* **2023**, *11*, 1158198, <https://doi.org/10.3389/fchem.2023.1158198>.
19. Ye, Q.; Zeng, Z.; Liang, X.; Li, W. Quercetin suppresses retinoblastoma cell proliferation and invasion and facilitates oxidative stress-induced apoptosis through the miR-137/FNDC5 axis. *Environ. Res.* **2023**, *237*, 116934, <https://doi.org/10.1016/j.envres.2023.116934>.
20. Homayoonfal, M.; Gilasi, H.; Asemi, Z.; Khaksary Mahabady, M.; Asemi, R.; Yousefi, B. Quercetin modulates signal transductions and targets non-coding RNAs against cancer development. *Cell Signal* **2023**, *107*, 110667, <https://doi.org/10.1016/j.cellsig.2023.110667>.
21. Asgharian, P.; Tazekand, A.P.; Hosseini, K.; Forouhandeh, H.; Ghasemnejad, T.; Ranjbar, M.; Hasan, M.; Kumar, M.; Beirami, S. M.; Tarhriz, V.; Soofiyani, S. R.; Kozhamzharova, L.; Sharifi-Rad, J.; Calina, D.; Cho, W.C. Potential mechanisms of quercetin in cancer prevention: focus on cellular and molecular targets. *Cancer Cell. Int.* **2022**, *22*, 257, <https://doi.org/10.1186/s12935-022-02677-w>.
22. Shahbaz, M.; Naeem, H.; Momal, U.; Imran, M.; Alsagaby, S.A.; Al Abdulmonem, W.; Waqar, A.B.; El-Ghorab, A.H.; Ghoneim, M.M.; Abdelgawad, M.A.; Shaker, M.E.; Umar, M.; Hussain, M.; Kumar, R.; Al Jbawi, E. Anticancer and apoptosis inducing potential of quercetin against a wide range of human malignancies. *Int. J. Food Prop.* **2023**, *26*, 2590–2626, <https://doi.org/10.1080/10942912.2023.2252619>.
23. Majumdar, G.; Mandal, S. Evaluation of broad-spectrum antibacterial efficacy of quercetin by molecular docking, molecular dynamics simulation and in vitro studies. *Chem. Phys. Impact* **2024**, *8*, 100501, <https://doi.org/10.1016/j.chphi.2024.100501>.
24. Luo, S.; Kang, X.; Luo, X.; Li, C.; Wang, G. Study on the inhibitory effect of quercetin combined with gentamicin on the formation of *Pseudomonas aeruginosa* and its bioenvelope. *Microb. Pathog.* **2023**, *182*, 106274, <https://doi.org/10.1016/j.micpath.2023.106274>.
25. Zhou, P.; Wang, L.; An, S.; Wang, C.; Jiang, Q.; Li, X. Fabrication of quercetin-loaded nanoparticles based on *Hohenbuehelia serotina* polysaccharides and their modulatory effects on intestinal function and gut microbiota in vivo. *Innov. Food Sci. Emerg. Technol.* **2022**, *78*, 102993, <https://doi.org/10.1016/j.ifset.2022.102993>.
26. Alizadeh, S.R.; Ebrahimzadeh, M.A. O-substituted quercetin derivatives: Structural classification, drug design, development, and biological activities, a review. *J. Mol. Struct.* **2022**, *1254*, 132392, <https://doi.org/10.1016/j.molstruc.2022.132392>.

27. Schüller, A.; Hähnke, V.; Schneider, G. SmiLib v2.0: A Java-Based Tool for Rapid Combinatorial Library Enumeration. *QSAR Comb. Sci.* **2007**, *26*, 407–410, <https://doi.org/10.1002/qsar.200630101>.
28. Release Notes: Release 2023-4. Available online: <https://www.schrodinger.com/life-science/download/release-notes/release-2023-4/> (accessed on 21 July 2024).
29. Cushnie, T.P.T.; Lamb, A.J. Recent advances in understanding the antibacterial properties of flavonoids. *Int J. Antimicrob. Agents* **2011**, *38*, 99–107, <https://doi.org/10.1016/j.ijantimicag.2011.02.014>.
30. Olivaro, C.; Paris, N.; M. Pía, C.; Vázquez, A. Antistaphylococcal Activity of Xanthium cavanillesii Lactones. *Pharmacogn. J.* **2014**, *6*, 39–42, <https://doi.org/10.5530/pj.2014.6.8>.
31. Hildebrand, J.H.; Benesi, H.A. Interaction of iodine with aromatic hydrocarbons. *Nature* **1949**, *164*, 963, <https://doi.org/10.1038/164963b0>.
32. Lanez, T.; Feizi-Dehnyabi, M.; Lanez, E. Assessment of the electrostatic binding of ferrocenylmethyl-nitroaniline derivatives to DNA: A combined experimental and theoretical study. *J. Mol. Struct.* **2024**, *1308*, 138386, <https://doi.org/10.1016/j.molstruc.2024.138386>.
33. Pires, D.E.V.; Blundell, T.L.; Ascher, D. B. pkCSM: Predicting Small-Molecule Pharmacokinetic and Toxicity Properties Using Graph-Based Signatures. *J. Med. Chem.* **2015**, *58*, 4066–4072, <https://doi.org/10.1021/acs.jmedchem.5b00104>.
34. Friesner, R.A.; Murphy, R.B.; Repasky, M.P.; Frye, L.L.; Greenwood, J.R.; Halgren, T.A.; Sanschagrin, P.C.; Mainz, D.T. Extra Precision Glide: Docking and Scoring Incorporating a Model of Hydrophobic Enclosure for Protein–Ligand Complexes. *J. Med. Chem.* **2006**, *49*, 6177–6196, <https://doi.org/10.1021/jm051256o>.
35. Morsy, S.; Morsy, A. Epitope mimicry analysis of SARS-COV-2 surface proteins and human lung proteins. *J Mol Graph Model* **2021**, *105*, 107836, <https://doi.org/10.1016/j.jmgm.2021.107836>.
36. Sharma, S.K.; Bangia, A.; Alshehri, M.; Bhardwaj, R. Nonlinear dynamics for the spread of pathogenesis of COVID-19 pandemic. *J. Infect. Public Health* **2021**, *14*, 817–831, <https://doi.org/10.1016/j.jiph.2021.04.001>.

## Publisher’s Note & Disclaimer

The statements, opinions, and data presented in this publication are solely those of the individual author(s) and contributor(s) and do not necessarily reflect the views of the publisher and/or the editor(s). The publisher and/or the editor(s) disclaim any responsibility for the accuracy, completeness, or reliability of the content. Neither the publisher nor the editor(s) assume any legal liability for any errors, omissions, or consequences arising from the use of the information presented in this publication. Furthermore, the publisher and/or the editor(s) disclaim any liability for any injury, damage, or loss to persons or property that may result from the use of any ideas, methods, instructions, or products mentioned in the content. Readers are encouraged to independently verify any information before relying on it, and the publisher assumes no responsibility for any consequences arising from the use of materials contained in this publication.